International Journal of Infrared and Millimeter Waves, Vol. 23, No. 8, August 2002 (© 2002)

A FUTURE MILLIMETER/SUB–MILLIMETER RADIOMETER FOR SATELLITE OBSERVATION OF ICE CLOUDS

Jungang Miao,[1] Thomas Rose,[2] Klaus Kunzi,[1] and Peter Zimmermann[2]

[1]*Institute of Environmental Physics*
University of Bremen
28334 Bremen, Germany
[2]*Radiometer Physics GmbH*
Birkenmaar St. 10, 53340 Meckenheim, Germany

Received May 10, 2002

Abstract: The instrument concept of a future spaceborne millimeter/sub–millimeter radiometer is proposed in this paper for the remote sensing of ice clouds from satellite. The proposed radiometer is expected to operate at a series of frequencies within the millimeter and sub–millimeter wave range from 150 to about 900 GHz. Five frequencies are selected in the atmospheric windows, i.e., 150, 220, 463, 683, 874 GHz, and at each frequency there are two orthogonally polarized channels. Three water vapor channels located close to 183.31 GHz are also included in this instrument, since they can provide water vapor information, which is needed for ice cloud parameter retrieval. To simplify system design and test, a modular design philosophy is followed in the receiver frontend design and two antennas are used separately for the millimeter and sub–millimeter channels. Overall, the instrument requirements can be met with today's technology, except for the channels at the highest frequencies, where the radiometric sensitivity can be larger than the required 1.0 K for the 10 km spatial resolution (2.5 ms integration time). However, this situation can be improved by averaging neighboring pixels in data processing if certain compromise in the spatial resolution can be made at these frequencies.

Keywords: Microwave radiometry, millimeter and sub–millimeter wave technology, satellite remote sensing of clouds.

1. Introduction

Atmospheric clouds play an essential role in the earth–atmosphere system. The importance of clouds for climate studies and weather forecast has long been recognized. However, our understanding to clouds is far from sufficient, especially in aspects such as the formation of ice clouds and their role in the global climate change [1]. To improve our understanding about the microscopic and macroscopic properties of ice clouds, appropriate measuring techniques are urgently needed, especially in a global scale. Satellite radiometry at millimeter and sub–millimeter wavelengths has been shown to be very effective in fulfilling this task [2,3]. The spaceborne radiometer proposed in this paper, CIWSIR (Cloud Ice and Water–vapor Sub–mm Imaging Radiometer), should fill the gap in providing ice cloud information, which is not available at present from ground–based, airborne or spaceborne instruments.

0195-9271/02/0800-1159/0 © 2002 Plenum Publishing Corporation

2. Instrument Requirements

2.1 Frequency Bands

Ice clouds are primarily composed of ice particles in different shapes and sizes, and they are usually located at the middle and high altitudes of the troposphere. In mm and sub–mm wavelengths, the interaction between atmospheric radiation and ice particles is dominated by scattering. The mm and sub–mm radiation of the atmosphere is mainly from water vapor, most of which is located in the lower altitude of the atmosphere. The atmospheric radiation from lower altitudes will be scattered off the path when propagating to a spaceborne radiometer through overlying ice clouds. This will result in a lower brightness temperature in the measurements of the spaceborne radiometer, compared with cloud–free cases. The brightness temperature difference between cloudy and clear–sky cases can be used therefore to extract information of ice clouds, e.g., the integrated ice water content, the ice particle characteristic size. Since the scattering effect of a typical collection of ice particles increases monotonically with the increase of frequency up to about 1000 GHz, it is a natural selection to have several frequencies spanning this range, in order to cover a wide range of particle size and cloud thickness. For CIWSIR, six frequencies from 150 to 900 GHz have been selected (for details on the rationale of frequency selection the interested reader is referred to [4]) and they are graphically shown in Figure 1.

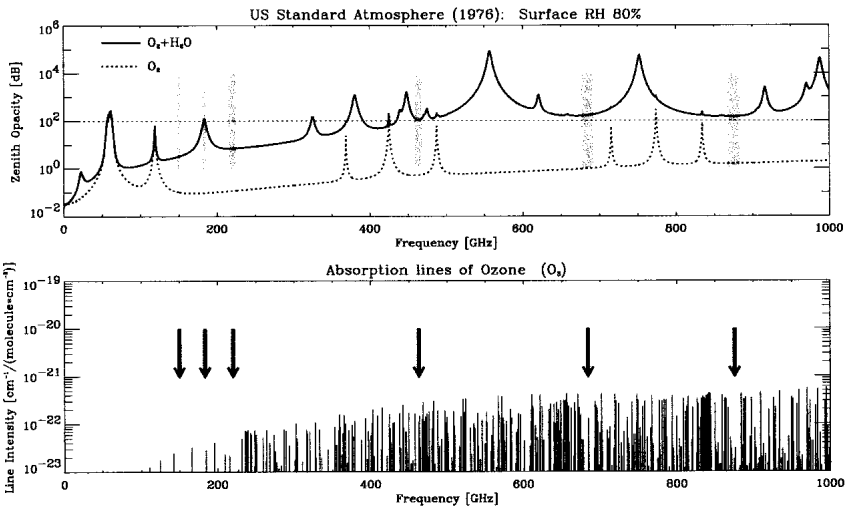

Figure 1: Locations of the proposed CIWSIR channels in the mm and sub–mm frequency range. Except for the 183 GHz case, the width of the gray bar indicates the approximate bandwidth of each channel. Together shown are the atmospheric opacity due to the absorption of water vapor and oxygen (upper panel) and the absorption line intensity of ozone (bottom panel).

Of the six frequencies, five are located at the atmospheric windows and three are in the sub–millimeter wave range. The passbands and the center frequencies of the three sub–mm channels are carefully selected, so that they avoid the considerable influence of atmospheric ozone emissions and, at the same time, they have a good match in weighting functions for clear sky situations. This means, the sub–mm channels measure essentially the same brightness temperature in clear sky conditions. The two mm wave channels (at 150 and 220.5 GHz) sound deeply down to the lower troposphere because of the relatively low absorption of water vapor at these two frequencies. Therefore, they are well suited to measure low and thick ice clouds [5]. The water vapor channels near 183 GHz consist of three channels, whose passbands are located symmetrically across the center frequency of 183.31 GHz (see Table 1 for details). This will enable us to measure the vertical distribution of water vapor in the atmosphere. Except for the water vapor channels, all window channels measure two orthogonal polarization simultaneously. All channels, including the water vapor channels, are operated in double sideband mode (DSB). The radiometric accuracy requirement is selected as 1.0 K r.m.s. (= relative accuracy, 1.5 K absolute accuracy) for all channels, which is related to the system noise temperature, T_{sys}, by

$$\Delta T = \frac{T_{sys}}{\sqrt{\tau B}}$$

for a total–power radiometer. Here, τ is the integration time, which is 2.5 ms for the conical scanning configuration of the given satellite, and B is the channel IF–bandwidth. Table 1 summarizes the radiometric requirements.

Table 1: Radiometric requirements of CIWSIR channels

Channel center [GHz]	IF–Bandwidth [GHz]	Integration time τ [ms]	Required max.T_{sys} [K]	Required ΔT
150.0	4.0	2.5	3150	1.0 @ 300K
183.31 ± 1.0	1.0	2.5	1600	1.0 @ 240K
183.31 ± 3.0	2.0	2.5	2200	1.0 @ 260K
183.31 ± 7.0	4.0	2.5	3150	1.0 @ 280K
220.5 ± 3.0	2.0	2.5	2200	1.0 @ 240K
462.5 ± 3.0	2.0	2.5	2200	1.0 @ 240K
683.0 ± 6.0	3.0	2.5	2700	1.0 @ 240K
874.0 ± 6.0	3.0	2.5	2700	1.0 @ 240K

2.2 Antenna Requirements

The main antenna requirements are determined by the scanning geometry of the radiometer (conical scanning at present), the satellites altitude (mean value of 830 km) and the required average footprint size (10 km for all frequencies). Figure 2 illustrates the dimensions and angles involved, which imply a half–power beam width (HPBW) requirement of 0.35°. According to diffraction theory, the effective antenna diameter must be no smaller than 400 mm to achieve the 0.35° HPBW at 150 GHz and with an antenna illuminating edge taper of –20 dB. For the sub–mm channels, antenna size reduces to 160 mm.

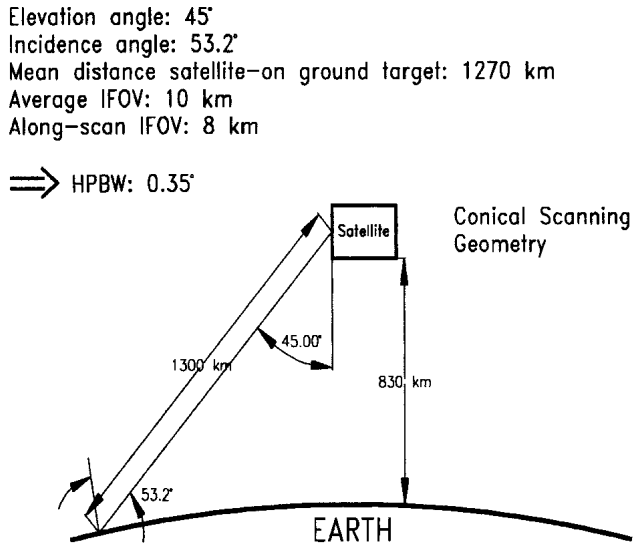

Figure 2: The conical scanning geometry of satellite and the implied main beam requirements.

3. Instrument Concept

The instrument design is carried out based on the idea that CIWSIR will be a stand–alone unit and the only interaction of it with other subsystems on the same satellite is performed by a purely digital data and command interface.

3.1. Instrument Configuration

Fig. 3 is a schematic diagram of the principal CIWSIR system layout. The basic concept is a complete optical separation of the mm and sub–mm channels and their associated calibration systems as well. This configuration has the following advantages:

- Improvement of redundancy for the calibration mirror and scanning motor. In the case of a calibration mirror failure only half of the CIWSIR channels are lost.
- Two ambient temperature calibration targets can be optimized for the different frequency ranges.
- The optical design of the quasioptical multiplexer is much easier. This also implies a lower beam distortion due to a reduced number of focussing elements.
- Two main reflectors. For imaging of the submm–beams a paraboloid reflector diameter of only 160 mm is necessary. The higher surface accuracy requirements for the submm–bands can be much more easily achieved with a smaller reflector.
- Illumination of two main reflectors offers more flexibility for the illumination angles. This reduces the number of elliptical mirrors in the quasioptical design.

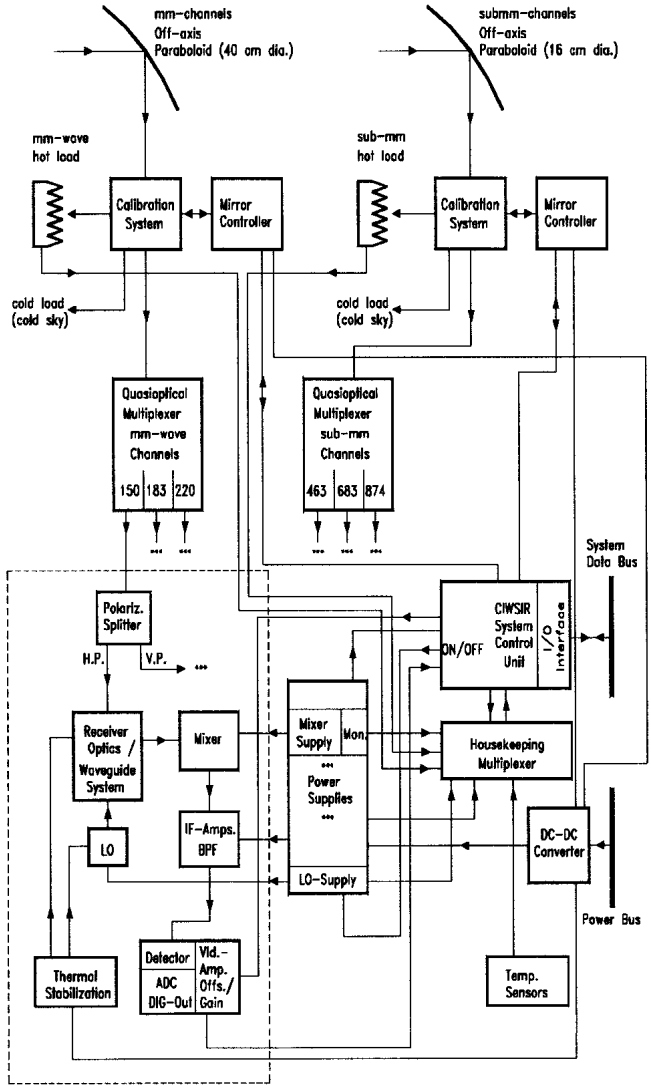
mm-channels
Off-axis
Paraboloid (40 cm dia.)
submm-channels
Off-axis
Paraboloid (16 cm dia.)
mm-wave
hot load
sub-mm
hot load
Calibration System
Mirror Controller
Calibration System
Mirror Controller
cold load
(cold sky)
cold load
(cold sky)
Quasioptical Multiplexer mm-wave Channels
150 183 220
Quasioptical Multiplexer sub-mm Channels
463 683 874
System Data Bus
Polariz. Splitter
H.P.
V.P.
CIWSIR System Control Unit
ON/OFF
I/O Interface
Receiver Optics / Waveguide System
Mixer
Mixer Supply
Mon.
Power Supplies
Housekeeping Multiplexer
LO
IF-Amps. BPF
LO-Supply
DC-DC Converter
Power Bus
Thermal Stabilization
Detector
ADC DIG-Out
Vid.-Amp. Offs./ Gain
Temp. Sensors

The basic working principle can be described as following. The beam coming from the paraboloid is reflected onto a calibration mirror (one for the 40 cm and the another for the 16 cm paraboloid) that can switch the radiometer's input either to the scene and or to the calibration loads (see Figs. 3 and 4). The calibration mirror is controlled in position and rotation direction by a compact controller module which itself is commanded from the CIWSIR system control unit (SCU). The calibration system output port is coupled to the input of a quasioptical multiplexer utilizing dichroic plates for frequency splitting. Since there are two distinct multiplexers they can be designed in a very compact way without the need for any refocussing mirrors. Each band is then split in polarization by a wire grid (except for the 183 GHz channels, where single polarization is required) and diplexed with a local oscillator beam (sub–mm channels only) into a mixer. The mixer's IF signal is amplified, filtered (band pass filter BPF) and finally detected.

The bias currents and voltages of all RF– and IF–components are monitored, to check for the system hardware status. Further housekeeping data is acquired by a number of temperature sensors that are distributed across the radiometer box (Gunn oscillators, receiver plates, hot load, power supplies, etc.). The various voltage signals are coupled to differential multiplexer inputs switched by the SCU. A 16 bit ADC converts the analog data to digital data which is then transferred to the system data bus via a bidirectional I/O–interface.

According to thermal analyses, a temperature variation of 40°C may occur during one satellite orbit. A thermal stabilization is foreseen for critical components (sub–mm LOs and detectors). The detector units will comprise a zero bias detector diode with associated RF matching network and subsequent DC low drift operational amplifiers. To improve the redundancy and to reduce spurious noise a 16 bit ADC is included in the detector circuit. Because of the high digitization resolution there is no need for a DC–amplifier's gain and offset control system. Only digitized data is sent from the detector to the SCU. An internal sampling clock (3.2 kHz) continuously initiates ADC conversions to guarantee a full 16 bit accuracy (gain stability of the ADC). The system power supply unit (SPSU) is powered by a low loss DC–DC converter / filter unit that is connected to the satellites power bus (28 V, DC).

3.2. Main Antenna Concept and Performance Evaluation

The main reflector of the antennas is selected to be a off–axis paraboloid. To achieve a nearly undistorted beam the focal length of the off–axis paraboloids is chosen to be about twice its diameter which leads to relatively narrow illumination angles. Table 2 summarizes the design parameters.

Table 2: The design parameters of the mm and sub–mm antennas

Paraboloid projected Ø [mm]	size [mm]	focal length [mm]	reflection angle	illumination angle	distance to phase center [mm]	surface accuracy [μm]
400	433 x 400	850	45°	11.96°	995.84	20
160	173 x 160	384	45°	10.55°	450.00	10

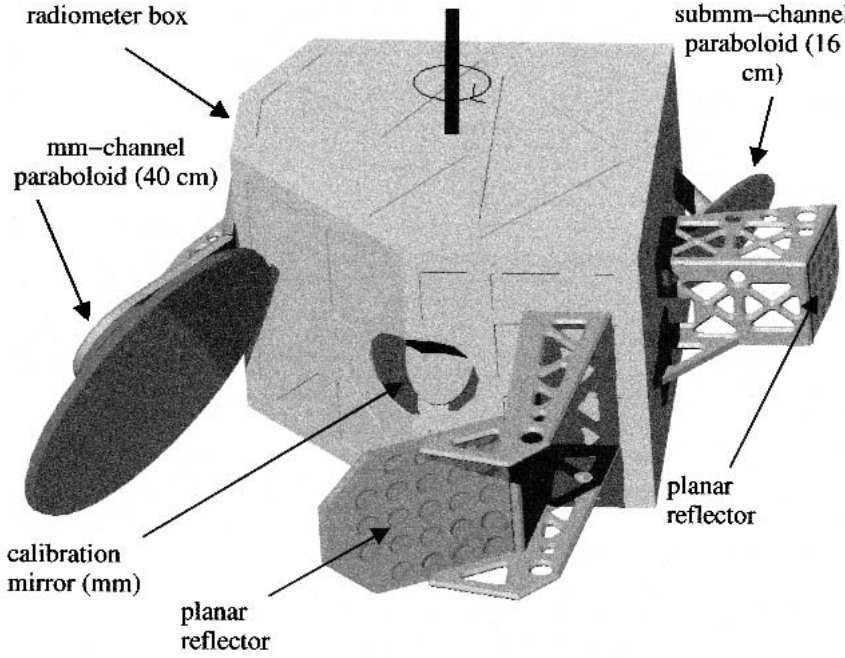

Figure 4: Compact CIWSIR layout with paraboloids and external planar mirrors for re–routing of paraboloidal beams. Also visible is the mm–wave calibration mirror. Both paraboloids are tilted relative to the horizontal plane by 22.5°. The rotation axis and direction are also shown.

Detailed optical performance analyses with a Gaussian beam illumination as input were carried out for the two antennas. The mm wave antenna beam patterns were found to match precisely at the −3 dB contour level, with HPBW = 0.36°, which corresponds to a footprint size of 8.4 km at 830 km satellite altitude, when viewed at 45° off nadir and with a viewing line distance to the earth of 1300 km for conical scanning. Only the 150 GHz beam shows a slightly broader pattern at lower power levels compared to the patterns at 183 and 220 GHz. The edge taper at 150 GHz is close to −20 dB while for the other two frequencies the taper is below −30 dB. For all frequencies the cross polarization is below 0.1% so that cross polarization is dominated by focussing elements of the internal quasioptic system. The paraboloid generates sidelobes below −30 dB. The optical performance of the sub–mm paraboloid is even better (with a size of 16 cm antenna). Table 3 summarizes the optical performance of both antennas. It is noted that the antenna aperture efficiency decreases with increasing frequency. This results from the system requirement of equal footprint size for all frequencies.

In order to achieve a compact system layout the beams between the paraboloids and their associated calibration mirrors have to be re–routed by external planar mirrors. This is also shown in Fig. 4.

Table 3: Optical performance of the two paraboloid configuration

f [GHz]	aperture efficiency	spillover loss	edge taper [dB]	2ω–Ø [mm]	sidelobe level [dB]	cross polarization
150	75%	1.52%	–19.5	535.8	–30.0	0.1%
183.3	46.2%	0.38%	–34.7	396.4	<–50	<0.05%
220.5	33.1%	0.15%	–51.3	329.3	<–50	<0.01%
462	46.5%	0.38%	–34	156.2	<–50	<0.05%
683	33.2%	<0.15%	–50	104.7	<–50	<0.01%
874	23.8%	<0.10%	<–60	81.0	<–50	<0.01%

3.3. Calibration System

Again, two independent calibration systems are proposed: one for the mm–wave channels and the another for the sub–mm channels. Each calibration system consists of a light weight planar calibration mirror and ambient temperature calibration target. The mirror is driven by a reliable 3–phase stepper motor (life time >6 years) with a step and settle time of <0.25 seconds. The stepper repeatability is <0.05°. The stepper controller accurately monitors the absolute mirror position and uses a reference position for initialization. The cold sky direction is rotated relative to the paraboloid antenna direction by 40° and the ambient temperature load is located at 140° so that the calibration mirror's total switching angle during calibration is only 180°. A minimization of this angle is necessary to optimize the total calibration time. With a rotation speed of one revolution in two seconds a calibration should be repeated every 5 to 10 revolutions with an integration time of 30 ms on each calibration target.

For the mm–wave cold sky view a direction between external planar mirror and paraboloid was selected to avoid problems with the beam divergence. The instrument rotation axis is centered to the minimum diameter envelope (1100 mm) (see Fig. 4).

The ambient temperature load is a pyramidal shaped absorber made from Ferrosorb CR–117 which is space approved. Its reflectivity should be <–30 dB. The physical temperature of the target is accurately monitored by a Pt–type precision sensor to ±0.1 K. The ambient temperature load is thermally isolated to reduce thermal gradients. An active temperature stabilization is not foreseen to avoid a temperature gradient between the radiating absorber surface and the absorber bulk material where the temperature is monitored. For an accurate calibration it is not important to keep the target temperature constant but it is necessary to know exactly the radiometric temperature. In such a way, the design is very compact and utilizes only two dichroic plates for each multiplexer.

3.4 Receiver Optics

The receiver optics basically consists of the following subgroups:

- frequency selective optics (quasioptical multiplexer QMux)
- focussing mirrors that transform the beams to match feedhorns or diplexers
- diplexer sections for the sub–mm channels.

Quasioptical Multiplexers: One of the reasons to select a two–paraboloid option for CIWSIR is the simplicity of the quasioptical multiplexers design that follows from the splitting into two independent multiplexers. Only four dichroic plates are needed (instead of five for the one paraboloid version). The 463 GHz beam is only reflected (not transmitted through a dichroic plate (DP)) by DPs so that optical transmission losses of the 463 GHz channels are reduced. The realization of the QMux is simpler since its design can be more compact.

Diplexers: For the sub–mm bands, fundamentally pumped mixers are used because of their higher sensitivity compared to subharmonic mixers and because of the non–availability of sufficient LO power for a subharmonic mixer in this frequency range. The disadvantage of the fundamentally pumped mixer is the higher effort for the optical part. Signal and LO beams have to be combined quasioptically by an interferometer with a wide IF bandwidth. The only possible selection for this application is a FFPI (Folded Fabry Perot Interferometer). For reasons of compactness and fabrication we selected the triangular FFPI version.

Modular Optics: For the CIWSIR optics a modular design philosophy was followed. The advantage is that alignments and tests can be performed on subunit level instead of handling a much more complicated system. In this way, the mm–wave optics and the sub–mm unit are nearly completely separated. Also, the sub–mm unit can be split into subsections for the different frequency bands as indicated in Fig. 5.

3.5 Receiver Concept

There are two types of receiver frontends that mainly differ in the quasioptical section and mixer operation. The sub–mm channels are based on a fundamental mode mixer that uses a LO frequency close to the signal frequency. The mixer LO power must be in the order of a few hundred μW. The LO– and signal–beams are superimposed by an interferometer. The fundamental mode mixer offers superior noise performance with feasible requirements in terms of LO power. The receiver diagram is illustrated in Fig.6. In the mm–wave regime subharmonic mixers meet the sensitivity requirements. In addition they have the advantage of a more simple front end design (waveguide system of LO and mixer, no diplexer needed) and a wider IF bandwidth. The mixer Schottky diode for a balanced design can be realized with a planar technology that offers repeatability and precision lithography for a good match of diode characteristics. For the sub–mm bands planar technology will be available in the future with probably similar sensitivity performance when compared to whisker contacted Schottky diodes. Another advantage of a planar structure is its mechanical stability.

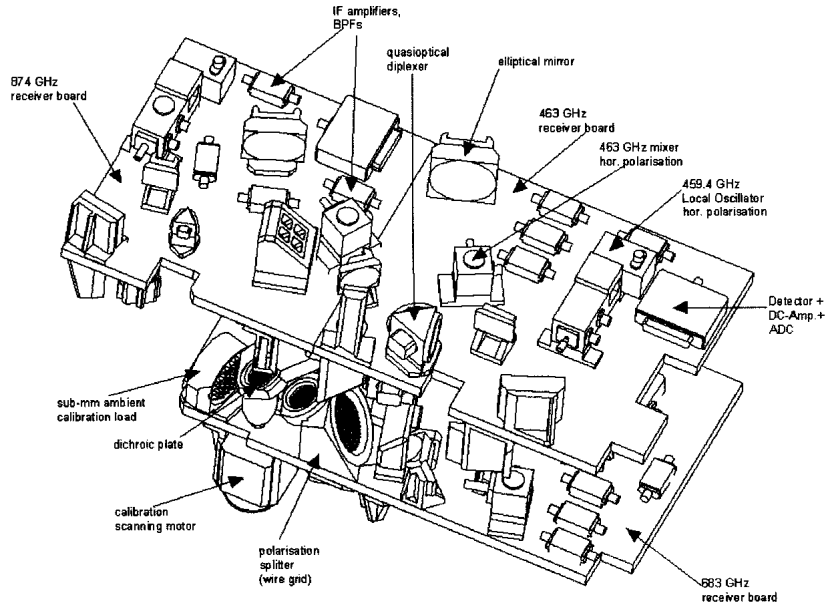

Figure 5: The sub–mm unit and its modular design splitting the unit into subsections for the three frequency bands. The orthogonal polarization is processed on the bottom of each board.

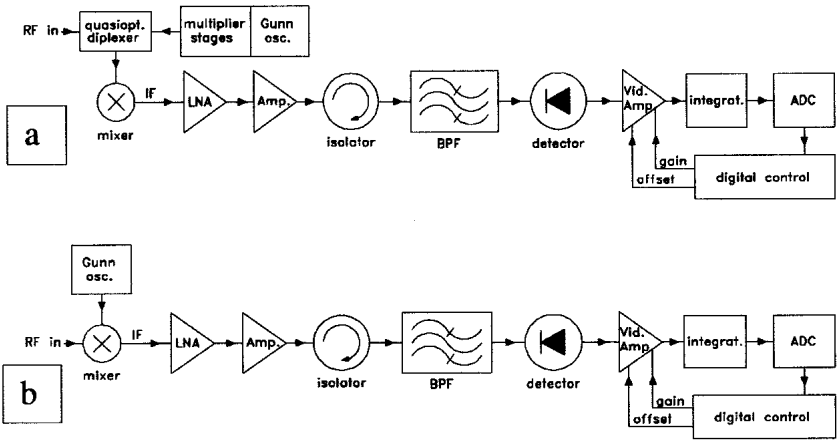

Figure 6: Receiver layout for sub–mm (a, fundamental mode mixer) and mm–wave (b, subharmonic mixer) channels. The receiver operation is double sideband mode (DSB).

The mixer IF is processed by a low noise amplifier which has an important impact on the system noise temperature. Its output signal is then further amplified to a power level of approximately –25 dBm which is ideal for the detector diode operation. The IF–amplifier chain must be isolated from the bandpass filter to match the amplifiers output impedance at frequencies that are rejected by the filter. The detected IF band power is transformed to a DC signal, amplified by low noise precision stabilized operational amplifiers and digitized by a 16 ADC that is contained in each detector unit.

The detector unit's output voltage is low pass filtered to define an integration time for the channel (2.5 ms). The ADC sampling rate is 8 times higher than the integration time (oversampling) to reduce digitization noise.

4. Conclusion and Summary on Instrument Performance

Quantitative measurements of ice clouds properties and climatology are urgently needed to understand major feedback in the Earth's climate. A mm and sub–mm radiometer is therefore proposed in this paper to provide the needed measurements from satellite in the future. We kept in mind in doing system design that this radiometer will be flying on low–orbit satellites and this radiometer should be a stand–alone instrument on the satellite. System requirements are thereby analyzed and an instrument concept has been developed.

Instrument performance analysis based on presently available technology shows that the basic system requirements to the radiometer can be generally met in all frequencies, except at the highest frequency end, where there is some difficulty to meet the 1 K radiometric sensitivity requirement at present. However, by properly relaxing the requirement on satellite spatial resolution (therefore the integration time), this requirement can also be achieved at the 683 and 874 GHz. And, this can be done in data processing by averaging the neighboring pixels. The overall instrument performance evaluation is summarized as following:

- Spatial Resolution: The summary of beam sizes is given in Table 5 for a mm–wave paraboloid of diameter 400 mm (850 mm focal length) and submm–wave paraboloid of diameter 160 mm (384 mm focal length) assuming a satellite–target distance of 1300 km (conical scanning geometry).

Table 5: Beam sizes for conical scanning geometry

Channel center ν [GHz]	Along track IFOV [km]	Along scan IFOV [km]	Average IFOV [km]	Polarization	HPBW [DEG]
150.0	13.0	8.0	10.0	H/V	0.35
183.31 ± 1.0	13.0	8.0	10.0	H	0.35
183.31 ± 3.0	13.0	8.0	10.0	H	0.35
183.31 ± 7.0	13.0	8.0	10.0	H	0.35
220.5 ± 3.0	13.0	8.0	10.0	H/V	0.35
462.5 ± 3.0	13.0	8.0	10.0	H/V	0.35
683.0 ± 6.0	13.0	8.0	10.0	H/V	0.35
874.0 ± 6.0	13.0	8.0	10.0	H/V	0.35

- Radiometric Performance: The radiometric performance of the CIWSIR channels is only determined by the system noise temperature T_{sys}, the IF–bandwidth B and the integration time τ by assuming that the receiver stability is sufficient (electronic instabilities must be smaller than the detector equivalent voltage for ΔT, the radiometric sensitivity). Table 6 reports the expected sensitivities for the various channels which are derived from already achieved system noise temperatures at or close to the CIWSIR channel frequencies.

Table 6: Radiometric performance of CIWSIR channels

Channel center [GHz]	IF–Bandwidth [GHz]	Integration time τ [ms]	T_{sys} [K]	required ΔT	expected ΔT
150.0	4.0	2.5	1900	1.0 @ 300K	0.6 @ 300K
183.31 ± 1.0	1.0	2.5	1900	1.0 @ 240K	1.1 @ 240K
183.31 ± 3.0	2.0	2.5	1900	1.0 @ 260K	0.9 @ 260K
183.31 ± 7.0	4.0	2.5	1900	1.0 @ 280K	0.7 @ 280K
220.5 ± 3.0	2.0	2.5	2000	1.0 @ 240K	0.9 @ 240K
462.5 ± 3.0	2.0	2.5	2000	1.0 @ 240K	0.9 @ 240K
683.0 ± 6.0	3.0	2.5	3300	1.0 @ 240K	1.2 @ 240K
874.0 ± 6.0	3.0	2.5	5500	1.0 @ 240K	2.0 @ 240K

Acknowledgment

This study was supported by the European Union under the contract of ENV4–CT98–0733.

References

1. K. N. Liou: Radiation and Cloud Processes in the Atmosphere. Oxford University Press, Oxford, 487pp., 1992.
2. K. F. Evans, S. J. Walter, A. J. Heymsfield, and M. N. Deeter, Modeling of Submillimeter Passive Remote Sensing of Cirrus Clouds, *J. Atmos. Sci.*, 37, 184–205, 1998.
3. J. R. Wang, G. Liu, J. D. Spinhirne, P. Racette, and W. Hart: Measurements of Cirrus Clouds with Airborne MIR, CLS, and MAS during FIRE III–ACE, *J. Geophys. Res.*, 106(D4), 15,251–15,263, 2001.
4. J. Miao, G. Heygster, and K. Kunzi: Ice Cloud and Background Water Vapor by Sub–MM and Very High Frequency MW Radiometry. *CLOUDS – A Cloud and Radiation Monitoring Satellite,* Final Report of EC Contract ENV4–CT98–0733, Appendix 7, 1999. (ftp://romatm9.phys.uniroma1.it/pub/clouds/report)
5. P. Racette, R. F. Adler, J. R. Wang, A. J. Gasiewski, D. M. Jakson, and D. S. Zacharias: An Airborne Millimeter–Wave Imaging Radiometer for Cloud, Precipitation, and Atmospheric Water Vapor Studies, *J. Atmos. Oceanic Technol.*, 13, 610–619, 1996.